



저작자표시-비영리-변경금지 2.0 대한민국

이용자는 아래의 조건을 따르는 경우에 한하여 자유롭게

- 이 저작물을 복제, 배포, 전송, 전시, 공연 및 방송할 수 있습니다.

다음과 같은 조건을 따라야 합니다:



저작자표시. 귀하는 원저작자를 표시하여야 합니다.



비영리. 귀하는 이 저작물을 영리 목적으로 이용할 수 없습니다.



변경금지. 귀하는 이 저작물을 개작, 변형 또는 가공할 수 없습니다.

- 귀하는, 이 저작물의 재이용이나 배포의 경우, 이 저작물에 적용된 이용허락조건을 명확하게 나타내어야 합니다.
- 저작권자로부터 별도의 허가를 받으면 이러한 조건들은 적용되지 않습니다.

저작권법에 따른 이용자의 권리는 위의 내용에 의하여 영향을 받지 않습니다.

이것은 [이용허락규약\(Legal Code\)](#)을 이해하기 쉽게 요약한 것입니다.

[Disclaimer](#)

**Development and validation of a visually explainable deep  
learning model for detection of C-shaped canals of the  
mandibular second molars in dental radiographs**

Sujin Yang

The Graduate School  
Yonsei University  
Department of Dentistry

**Development and validation of a visually explainable deep  
learning model for detection of C-shaped canals of the  
mandibular second molars in dental radiographs**

Sujin Yang

The Graduate School

Yonsei University

Department of Dentistry

**Development and validation of a visually explainable deep  
learning model for detection of C-shaped canals of the  
mandibular second molars in dental radiographs**

A Dissertation

Submitted to the Department of Dentistry  
and Graduate School of Yonsei University

in partial fulfillment of the  
requirements for the degree of  
Doctor of Philosophy in Dentistry

Sujin Yang

June 2021

This certifies that the Dissertation of Sujin Yang is approved.

---

Thesis Supervisor : Kee-Deog Kim

---

Thesis committee member #1 : Bock-Young Jung

---

Thesis committee member #2 : Wonse Park

---

Thesis committee member #3 : Nan-Sim Pang

---

Thesis committee member #4 : Hwiyoung Kim

The Graduate School  
Yonsei University

June 2021

## 감사의 글

석박사 통합과정을 진행하면서 저의 학위논문이 잘 마무리될 수 있기까지 많은 분들의 도움이 있었습니다. 이 글을 통해 감사의 인사를 드리고자 합니다.

좋은 연구의 기회를 주시고 연구자로서 앞으로 나아가야 할 길에 대해 지도해주신 김기덕 교수님 감사합니다. 저의 연구에 새로운 방향을 제시해 주시고 마지막까지 큰 그림을 그릴 수 있게 지도해주신 박원서 교수님 감사합니다. 바쁘신 중에도 꼼꼼하고 면밀하게 논문의 심사를 맡아주신 정복영 교수님 감사합니다. 매학기 유익한 가르침을 주시고 진심어린 조언을 해 주신 방난심, 정지은 교수님 감사합니다. 또한 생소한 분야의 연구를 하는 제게 연구과정과 학위논문 작성 과정에서 아낌없는 조언을 해 주신 김휘영 교수님 감사합니다.

박사학위 논문을 마무리 하며 돌이켜보면, 병원 생활과 연구, 논문 진행에 힘들고 어려운 일이 많았던 중 스스로 열심히 살았다고 느끼면서도, 어느 하나 완벽히 해내지 못한 것 같아 마음 한켠이 무거울 때가 있습니다. 이처럼 모자란 저조차 이렇게 잘 올 수 있기까지는 사랑하는 가족과 병원 동료들의 도움이 매우 컸습니다. 늘 응원해주며 제 긴 공부를 기다려주신 부모님, 감사하고, 사랑합니다. 이 두 마디의 말로 충분하지 않겠지만, 사랑하고 존경하는 부모님께 이 박사학위 취득의 영광을 돌리고 싶습니다.

연구를 진행할 때 바쁘지만 실험을 같이 도와준 선생님들께도 모두 감사드립니다. 많은 자료 정리에 함께 힘써주신 김재연 선생님 감사합니다. 또한, 딥러닝 학습모델 개발을 위해 바쁜 일정에도 코딩에 힘써주신 이하경, 장병한 선생님 감사합니다.

지면으로 미처 언급하지 못했지만, 저를 아끼고 격려해 주셨던 모든 분들께 진심으로 감사하다는 말씀을 전합니다. 더욱 정진하며 바른 모습으로 한층 성장해 치의학 보건 분야에서 꼭 필요한 존재가 되도록 노력하겠습니다.

2021년 6월  
양수진 올림

# Table of Contents

List of Figures .....	ii
List of Tables .....	iv
Abstract .....	v
I. Introduction .....	2
II. Material and Methods .....	5
2.1. Data collection .....	5
2.2. Ground truth annotation .....	8
2.3. Data preparation .....	9
2.4. CNN model training and evaluation .....	10
2.5. Statistical analysis .....	12
III. Results .....	13
IV. Discussion .....	25
V. Conclusion .....	32
References .....	33
국문요약 .....	38

## List of Figures

Figure 1. Multiclass classification confusion matrixes drawn from the results. The diagonal elements are the number of points where the predicted label matches the real label, while the non-diagonal elements show the wrong detections made by the classifier. The higher the diagonal value and the darker the shade of peach, the more accurate the diagnosis.

Figure 2. ROC curves for each of the groups obtained using periapical, panoramic, or both radiographs from the crown and root group or root only group. The p-values obtained between the crown and root group and root only group using periapical images, panoramic images, and both images were 0.101, 0.027, and 0.036 respectively. (The level of significance was set at  $p < 0.05$ .)

Figure 3. Radiograph examples and activation maps from the periapical or panoramic radiograph, from the crown and root group or root only group. The radiographic images were normalized, then Class Activation Map(CAM)s were drawn by applying Grad-CAM, and guided Grad-CAM. Heatmaps are focused in the apical one third portion of the tooth; however, in some cases the additional heatmaps are positioned near the pulp chamber area. (Note the heatmap focusing

on the coronal one third on the panoramic radiograph example of the C shaped canal from the grown & root group.)

Figure 4. An overview of the expanded deep learning model and feedback process from real world data.

## List of Tables

Table 1. Study population and baseline characteristics of the patients and teeth included in the study.

Table 2. Prediction performance on periapical, panoramic, or both radiographs of the crown and root group or root only group.

**ABSTRACT**

**Development and validation of a visually explainable deep  
learning model for detection of C-shaped canals of the  
mandibular second molars in dental radiographs**

Sujin Yang

*Department of Dentistry*

*The Graduate School*

*Yonsei University*

Directed by professor Kee-Deog Kim, D.D.S., M.S.D., Ph.D.

The purpose of this study was of this study was to develop and validate of a visually explainable deep learning model for detection of C-shaped canals of the mandibular second molars in dental radiographs.

The periapical, panoramic, and CBCT images of 1000 mandibular second molars were collected from 372 patients. The diagnostic performance of the deep learning system using periapical and panoramic radiographs was investigated in respect to its ability to determine whether the second mandibular molar showed a C shaped canal configuration. The results of the canal configuration on CBCT were used as a gold standard.

The AUC of the crown and root group was 0.96(periapical), 0.92(panoramic), 0.95(total) and the root only group was 0.97(periapical), 0.96(panoramic), 0.99(total). The sensitivity of the crown and root group was 0.93(periapical), 0.83(panoramic), 0.88(total) and the root only group was 0.83(periapical), 0.92(panoramic), 0.98(total). The specificity of the crown and root group was 0.91(periapical), 0.86(panoramic), 0.89(total) and the root only group was 0.93(periapical), 0.85(panoramic), 0.99(total). The deep CNN algorithm model showed high accuracy in predicting the C-shaped canal variation among mandibular second molars. With further optimization of the test data using a larger dataset and

improvements made in the model, a deep learning system can be expected to effectively diagnose C-shaped canals and aid clinicians in everyday practice.

---

Keywords: Artificial intelligence, Deep learning, Canal morphology, Mandibular second molar, C-shaped canal

**Development and validation of a visually explainable deep  
learning model for detection of C-shaped canals of the  
mandibular second molars in dental radiographs**

Sujin Yang

*Department of Dentistry*

*The Graduate School*

*Yonsei University*

Directed by professor Kee-Deog Kim, D.D.S., M.S.D., Ph.D.

## 1. Introduction

Knowledge of the root shape and root canal configuration is essential for the successful outcomes of surgical and non-surgical root canal treatment.<sup>1 2</sup> However the anatomy of the root and canal systems can be difficult to judge from a two-dimensional radiograph, and in many cases the reading of a periapical radiograph is a part which requires experience and mastery of the clinician.<sup>3</sup> This is especially important in cases of treating the mandibular second molar which show a high prevalence of C-shaped root canals. Many studies have reported the prevalence of C-shaped canals to differ among different ethnic groups, with the prevalence among Asians reported to be the highest being 10~45%.<sup>4 5 6 7</sup> The C-shaped canal variation shows a complex canal system compared to the 3 canal system usually found in Caucasians<sup>8</sup> and lead to challenges in canal debridement, disinfection and obturation.<sup>9</sup>

Since the complex anatomic feature of the root renders periodontic as well as endodontic treatment and maintenance a difficult task, it is important for the clinician to accurately evaluate the root and canal morphology.<sup>10</sup> For this matter cone-beam computed tomography (CBCT) is applied as the gold standard for evaluating such features. CBCT produces 3 dimensional images which are free of problems commonly found in conventional radiographs such as superimposition or

image distortion and is reported to show high diagnostic accuracy similar to that obtained from conventional CTs while having lower radiation doses.<sup>11</sup> Nonetheless since CBCT examinations still result in high radiation doses compared to conventional panoramic or periapical radiographs, this cannot be readily applied to all patients unless there exists another particular indication for a requisite CBCT, i.e., an adjacent impacted third molar that is in need of extraction and shows proximity to the inferior alveolar nerve.

In the recent decade artificial intelligence (AI) has actively been introduced and applied in dentistry. Convolution Neural Networks (CNNs) have shown excellent performances in computer vision, yielding promising results in terms of detection and classification of certain diseases in the radiological and pathological field. The deep learning-based CNN models report high accuracy and efficiency and prove its potential to be implemented in various clinical situations such as detection of diseases such as dental caries<sup>12</sup>, periodontitis<sup>13</sup>, osteoporosis<sup>14</sup>, and TMJ osteoarthritis<sup>15</sup>. Additionally, CNN models have become interpretable, and has at the least overcome its un-explainability to a certain level through the application of GRAD-CAM, which visualizes class activation maps<sup>16</sup> highlighting regions contributed to the model's decision. Applying this deep learning system to the detection of root canal variations using conventional radiographs would prove effective for the successful treatment and management outcomes. Accordingly, the

purpose of this study was to develop and validate a visually explainable deep learning model for the detection of C-shaped canals of the mandibular second molars in dental radiographs.

## 2. Material and Methods

### 1. Data collection

The images were retrospectively selected and collected from a database of patients who visited Yonsei University Dental Hospital, Department of Advanced General Dentistry between October 2018 and October 2020 for extraction of wisdom teeth in the posterior mandible area. The patients had undergone a basic screening of panoramic radiographs and periapical radiographs in the second molar areas, and an additional dental CBCT examination was done for identification of the impacted third molars. A total of 401 patients were included, and in the process, 31 patients were excluded because of blurred images due to patient movement during radiograph taking, cropped images of teeth not showing the entire tooth and other minor problems such as non-anatomic Patient cohort consisted of 162 males and 208 females, with an age range of 17~62 years (median 26 years; mean age  $28.45 \pm 9.24$  years). The study population and baseline characteristics of the patients and teeth included in the study are described in Table 1.

Table 1. Study population and baseline characteristics of the patients and teeth included in the study.

Patient		Non C	Event	C	Total
Subject factors					
Age	<30	186		125	311
	≥30	43		16	59
sex	Male	98		64	162
	Female	114		94	208
Tooth					
Subject factors			Event		Total
Age	<30	218		255	473
	≥30	120		123	243
Sex	Male	167		139	306
	Female	239		171	410

CBCT images were taken in a standard upright position on RAYSCAN Alpha plus (RAYSCAN Alpha plus; Ray Co., Hwaseong, Korea) or Pax-Zenith 3D (Pax-Zenith; Vatech Co., Hwaseong, Korea) with the following parameters: scanning time, 14 s; field of view,  $100 \times 100$  cm; tube voltage, 90 kVP; tube current, 12 mA; and voxel size, 0.18, based on the patient's size) on the scanning device.

Panoramic images were obtained using Pax-i plus (Pax-I Plus; Vatech Co., Hwaseong, Korea) with the standard parameters, including a tube voltage of 73 kV, tube current of 9 mA, and acquisition time of 13.5 s. Periapical images were obtained under a tube voltage of 60 kV, tube current of 7 mA, with acquisition time of 0.125 seconds.

This study was approved by the institutional review board of Yonsei University Dental Hospital. (Approval number: 2-2020-0076)

## 2. Ground truth annotation

The diagnostic performance of the deep learning system using periapical and panoramic radiographs was investigated in respect to its ability to determine whether the second mandibular molar showed a C shaped canal configuration. The results of the canal configuration on CBCT were used as the ground truth.

Image patches were prepared by first anonymizing the information of the patient's name, gender, age, and patient number. Then the image was cropped by drawing a bounding box from either the periapical images or the panoramic images to contain the crown and root of the second molar area or only the root portion of the second molar. These cropped images were sorted as "crown and root" or "root only" groups. The images were then adjusted to a  $300 \times 400$  pixel size for "crown and root" or  $300 \times 300$  pixel size with a resolution of 96 pixel per mm and saved in BMP (Bitmap) format image file using PhotoscapeX software. (ver.4.1 MOOII Tech.)

The prepared images were then reviewed and classified into two categories: "non-C" referring to non-C shaped or "C" referring to C-shaped, by a dentist with expertise of over 5 years and using the CBCT data as ground truth (GT). The Federation Dentaire Internationale (FDI) teeth numbering system (ISO-3950) was used, labeling the left mandibular second molar as no. 37 and the right mandibular second molar as no. 47.

### 3. Data preparation

Data augmentation techniques were applied to prevent overfitting owing to the small dataset size. Augmentation was performed with rotation, horizontal flip or altering the contrast, brightness, and sharpness of the prepared images. The images were resized to (224, 224) and a rotation angle from  $-1^\circ$  to  $1^\circ$  in  $0.5^\circ$  increments and a gamma range from 0.7 to 1.3 in increments of 0.3 were used for the rotation and gamma correction, respectively. The average and standard deviation of pixel values for the entire data were used for image normalization. The total number of images increased by 3 times, and a total of 3000 periapical, 3000 panoramic, and 6000 images in total were included. The dataset was randomly divided into training, validation, and testing sets in a ratio of 8:1:1.

#### 4. CNN model training and evaluation

EfficientNet was utilized as the CNN model for this study due to its efficiency and high-performance for image classification. EfficientNet proves to show high performance in transfer learning because it starts from a mobile-sized baseline network developed from an automated machine learning (Auto-ML) framework named EfficientNet-B0, and the compound scaling method is used to scale up the accuracy<sup>17</sup>. This allows for the reduction the training time and the number of images required to create a suitable classifier.

The model was optimized by stochastic gradient descent method with the weight decay and momentum of 0.0001 and 0.9, respectively. Categorical cross-entropy was used as the loss function for training, and RMSprop was used as the optimizer. The training was performed for 400 epochs. The learning rate and the batch size was set to 0.00002 and the batch size was set to 32, respectively.

This model was implemented on a system with CPU Intel(R) Xeon(R) CPU E5-2690 v4 @ 2.60GHz, RAM 252GB (264037304KB), and GPU Tesla V100 NVIDIA, USA. Pytorch version 1.7.0 with CUDA 10.1 on Ubuntu 18.04 was used.

The accuracy, sensitivity (recall), specificity, positive predictive value (PPV; or precision), and negative predictive value, F1-score, time for training and time for testing of the deep learning system were calculated in respect to the gold standard

CBCT results. The area under the curve (AUC) was also evaluated from the receiver operating characteristic (ROC) analysis.

## 5. Statistical analysis

Diagnostic performances were compared using the Mann-Whitney U Test. The AUC values were compared using McNemar's chi-square analysis. The level of significance was set at  $p < 0.05$ .

### 3. Results

The results of six groups were obtained respectively and compared. The results were primarily divided into two groups; by the image used containing both the coronal and root portion (crown and root group) or only the root portion (root only group). Then each group was divided by the source of the image data used; the source being from only the periapical images (periapical group), only from the panoramic images (panoramic group), or both images (total group). The validation loss dropped from 0.29 to 0.17 after 400 training epochs.

The AUC of the crown and root group obtained by using only periapical radiographs (periapical group), only panoramic radiographs (panoramic group) or both images(total) group was 0.96, 0.92, 0.95 respectively. The AUC of the root only group obtained by using only periapical radiographs (periapical group), only panoramic radiographs (panoramic group) or both images (total) group was 0.97, 0.96, 0.99 respectively. The sensitivity of the crown and root group was 0.93 (periapical), 0.83 (panoramic), 0.88 (total) and the root only group was 0.83 (periapical), 0.92 (panoramic), 0.98 (total). The specificity of the crown and root group was 0.91 (periapical), 0.86 (panoramic), 0.89 (total) and the root only group was 0.93 (periapical), 0.85 (panoramic), 0.99 (total). The accuracy, sensitivity (recall), specificity, positive predictive value (PPV; or precision), and negative

predictive value, F1-score, time for training of the model for each group are shown in Table 2.

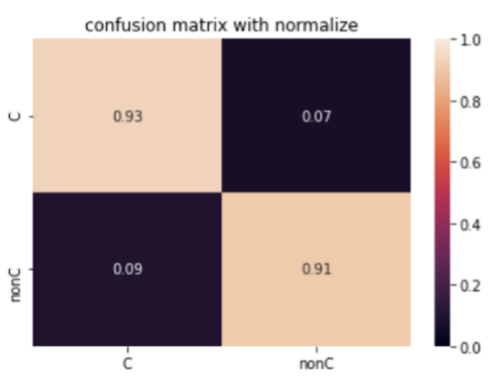
Table 2. Prediction performance on periapical, panoramic, or both radiographs of the crown and root group or root only group.

	Crown and root group			Root only group		
	Periapical	Panoramic	All images	Periapical	Panoramic	All images
Accuracy	0.92	0.85	0.89	0.88	0.89	0.98
Sensitivity (Recall)	0.93	0.83	0.88	0.83	0.92	0.98
Specificity	0.91	0.86	0.89	0.93	0.85	0.99
Positive Predictive Value(Precision)	0.93	0.79	0.91	0.92	0.88	0.99
Negative Predictive Value	0.83	0.89	0.86	0.85	0.9	0.97
F1-score	0.93	0.81	0.9	0.87	0.9	0.98
AUC	0.96	0.92	0.95	0.97	0.96	0.99
Time for training	44m 14s	27m 19s	56m 15s	39m 58s	32m 31s	48m 49s

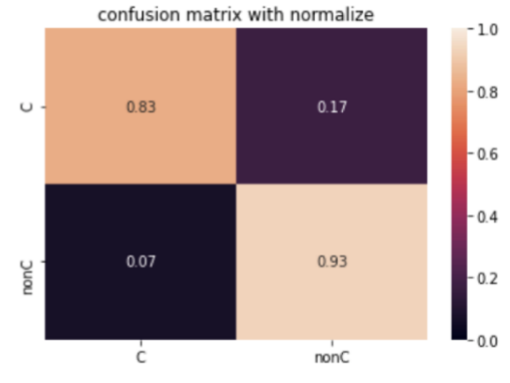
The AUC Multiclass classification confusion matrices are shown in Figure 1.

The  $p$ -values obtained between the crown and root group and root only group using periapical images, panoramic images, and both images were 0.101, 0.027, and 0.036 respectively, the panoramic group and both group showing statistical significance.

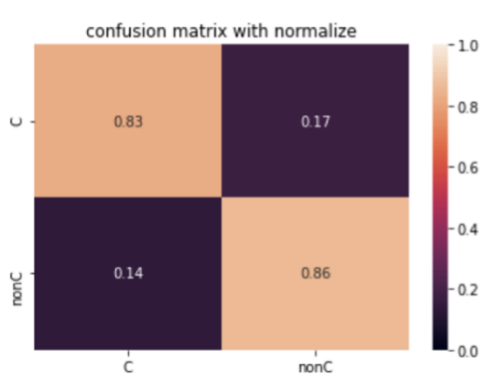
**Crown and root, periapical only**



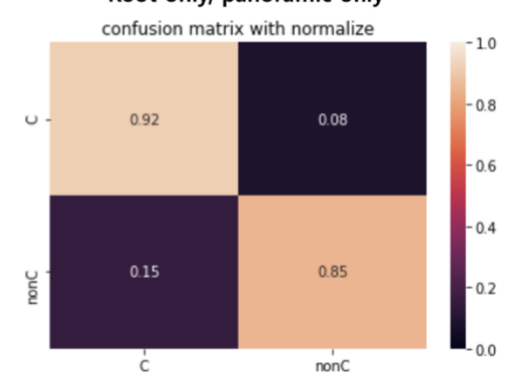
**Root only, periapical only**



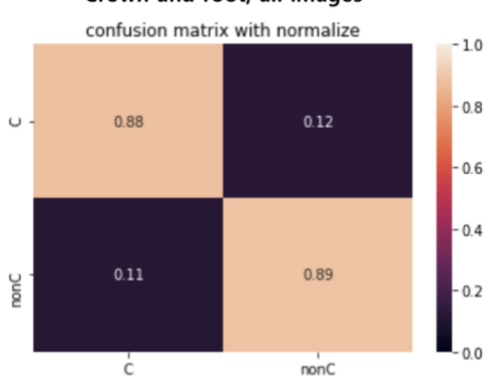
**Crown and root, panoramic only**



**Root only, panoramic only**



**Crown and root, all images**



**Root only, all images**

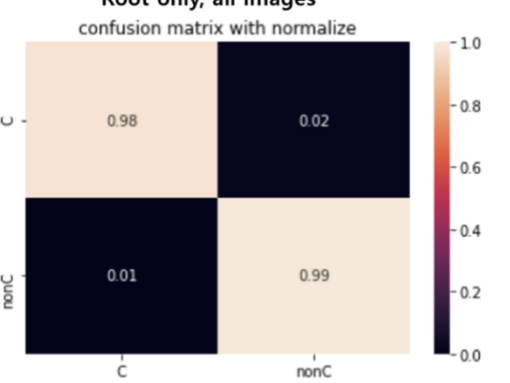


Figure 1. Multiclass classification confusion matrixes drawn from the results. The diagonal elements are the number of points where the predicted label matches the real label, while the non-diagonal elements show the wrong detections made by the classifier. The higher the diagonal value and the darker the shade of peach, the more accurate the diagnosis. The  $p$ -values obtained between the crown and root group and root only group using periapical images, panoramic images, and both images were 0.101, 0.027, and 0.036 respectively, the panoramic group and both group showing statistical significance.

The ROC curves and AUC of each group are shown in Figure 2.

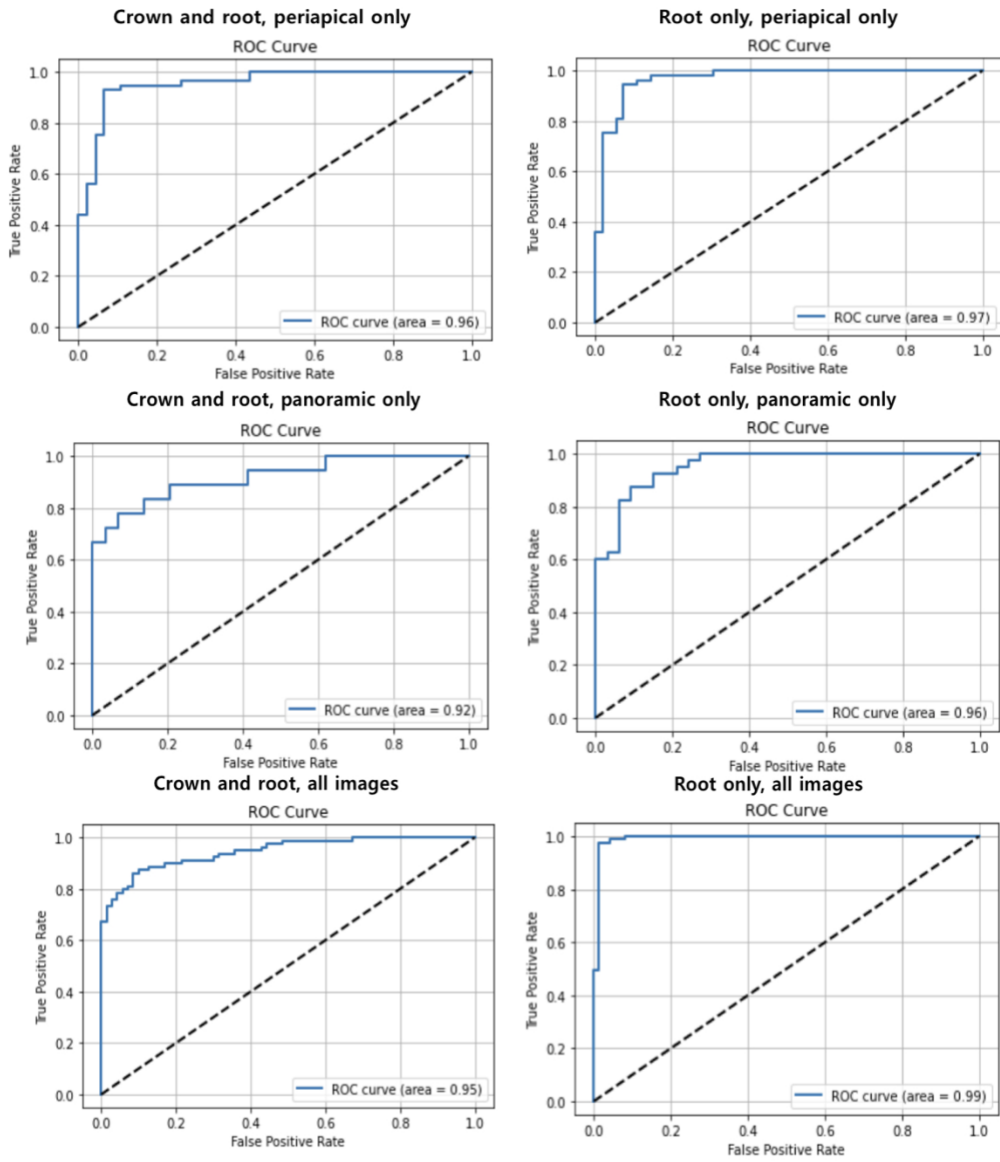
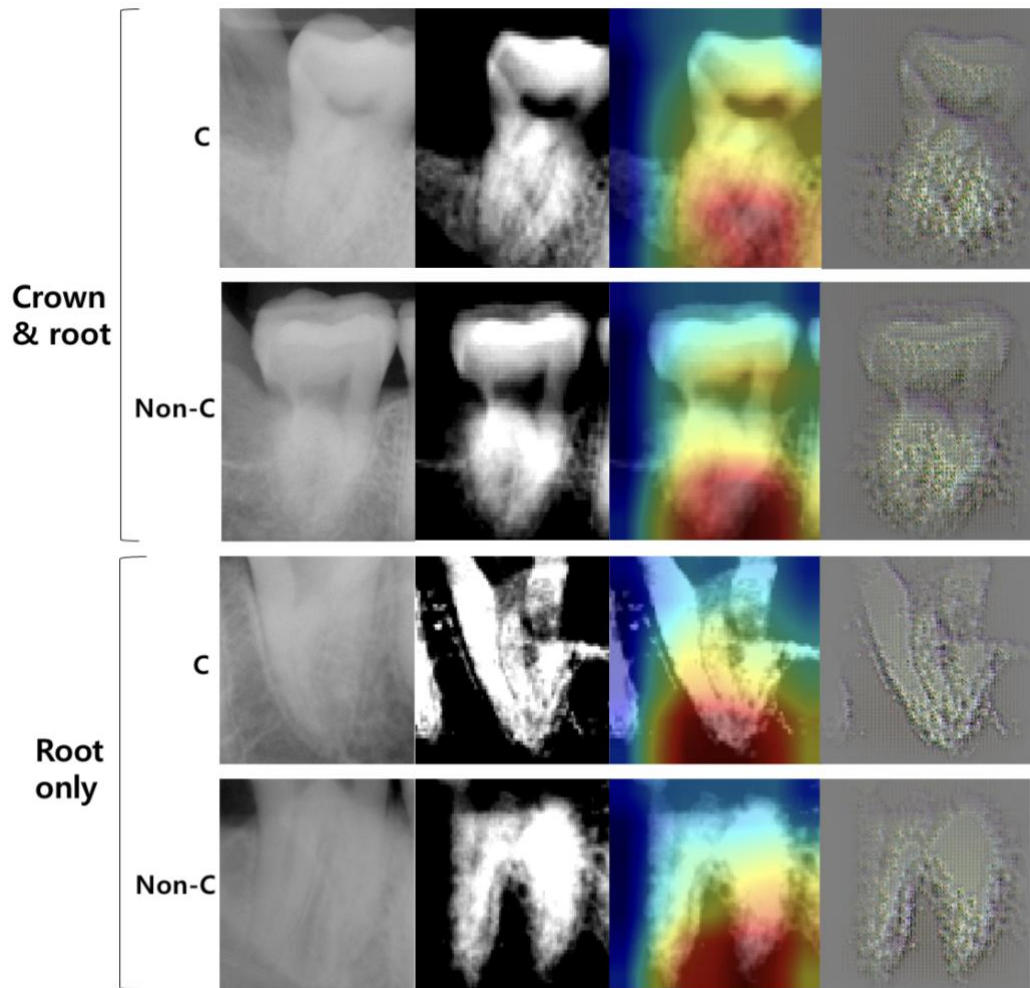


Figure 2. ROC curves for each of the groups obtained using periapical, panoramic, or both radiographs from the crown and root group or root only group. The p-values obtained between the crown and root group and root only group using periapical images, panoramic images, and both images were 0.101, 0.027, and 0.036 respectively, each showing statistical significance. (The level of significance was set at  $p < 0.05$ .)

To compare model performance based on the human perception and add interpretability to the model, Guided Grad-CAM was applied to show visualized class activation map (CAM)s upon the crown or root within the radiographic image. Most CAMs highlighted the root portion area, and especially the apical 1/3 area. However, in some cases the highlights were represented in Cemento-Enamel Junction (CEJ) areas and such misinterpretations were more frequently found in the crown and root group. The examples of Grad-CAM and guided Grad-CAM of the “C” and “non-C” using “crown and root” or “root-only” obtained from periapical, panoramic, or both radiographs are shown in Figure 3.

Periapical radiograph



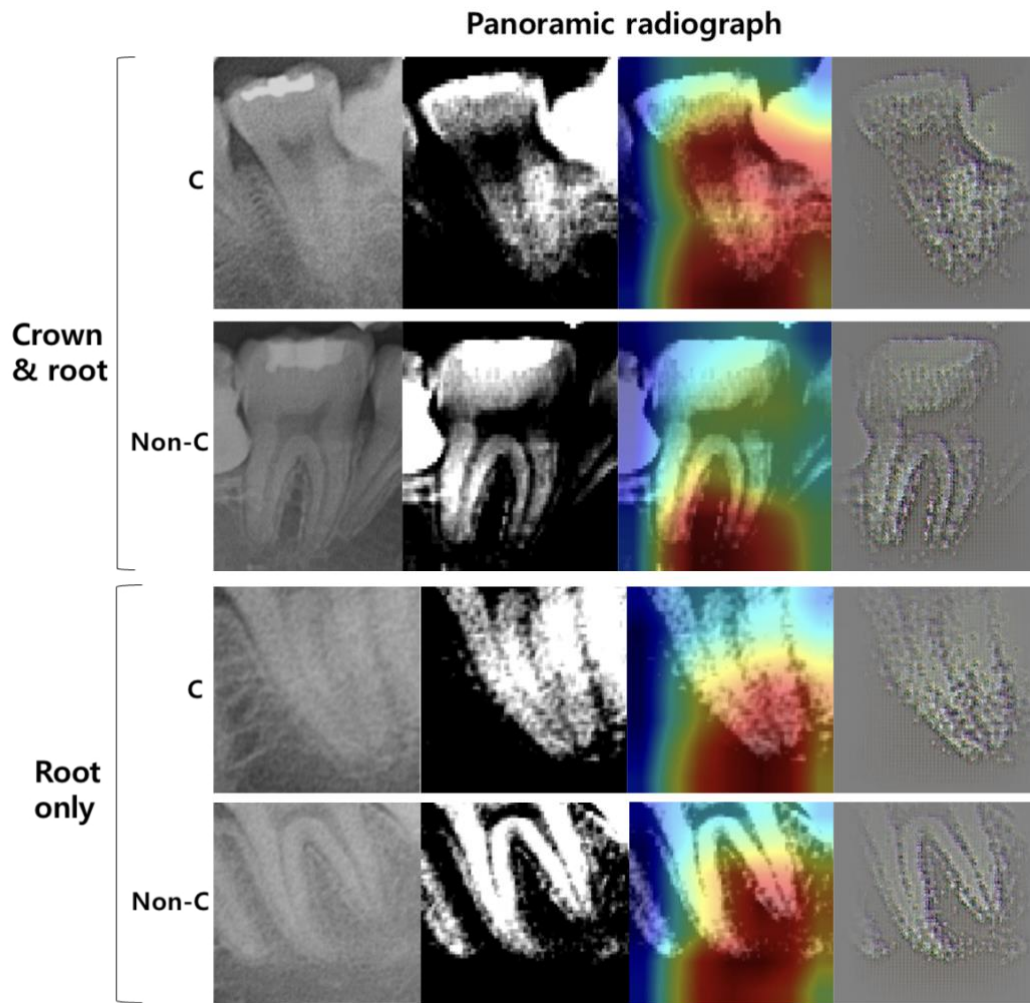


Figure 3. Radiograph examples and activation maps from the periapical or panoramic radiograph, from the crown and root group or root only group. The radiographic images were normalized, then Class Activation Map (CAM)s were

drawn by applying Grad-CAM, and guided Grad-CAM. Heatmaps are focused in the apical one third portion of the tooth; however, in some cases the additional heatmaps are positioned near the pulp chamber area. (Note the heatmap focusing on the coronal one third on the panoramic radiograph example of the C shaped canal from the grown & root group.)

#### 4. Discussion

Contrary to the fact that deep learning systems have been actively applied and implemented to various medical fields, they have not yet taken place in routine dental practice. This is a surprising result when acknowledging that dentistry is especially suited to apply AI tasks due to its abundance in image data of a particular anatomic region from different time points, amply accompanied non-imagery data such as clinical records, along with the prevalence of dental diseases among patients.

<sup>18</sup> When deep learning is applied to the endodontic field it can likewise prove as a powerful tool in supportive guidance to diagnosis, endodontic treatment and follow-up management. Specifically, if the root canal morphology could be predicted on panoramic or periapical radiographs before endodontic treatment, it would be possible to preemptively identify those patients who require meticulous canal debridement and sealing, ask for an additional CBCT taking to evaluate the specific root canal morphology (since it is not possible to perform CBCTs on all patients undergoing root canal treatment), and warn the patient of possible outcomes due to the complexity of the root and canal anatomy.

In this study, diagnostic performance from using only the periapical radiographs were slightly higher than those from the panoramic radiographs and using both images showed similar or higher results compared to the periapical groups. Periapical radiographs generally have better image quality and is frequently taken

in the clinical background to focus on a particular tooth number. The periapical radiographs used in this study were not taken in a fixed angle because they were taken before or after mandibular third molar extraction where the third molar is put upon the center of the radiograph rather than the second molar. However, this did not appear to hinder the diagnostic performance of the model. Panoramic images also show uncertainties due to image magnification or ghost images. The results imply that the accumulated image distortion was greater in the panoramic radiographs. In some clinical situations, panoramic images can be more helpful to the dentist or radiologist when detecting the C shaped canal of the mandibular second molar because there is less rotation of the tooth when the image is taken, alongside the fact that the opposite side tooth can be compared. This did not act upon the model's performance since the image was cropped in advance, however, this should be regarded in further studies where the mandibular second molar is first detected in the panoramic radiograph and then classified as whether it has a C-shaped canal variation. Also, the performance was higher when only the root portion of the tooth was used for training. This is presumably the aftermath of the overlapping of various prostheses in the crown portion such as inlays or crowns. Without the crown portion we could minimize the chances in which the anatomy or prosthesis of the crown portion interferes with the root portion or chances the CNN model mistakenly focuses on the coronal portion of the tooth for root canal

classification. In further studies, by adding an object detection model that can detect and crop the area of the second mandibular molar root to the classification algorithm, we may be able to build a further efficient model fit for this task.

Efficient Net was chosen among the many proposed deep learning algorithms for this study because it is a state-of-the-art CNN model that set records in both accuracy and computational efficiency.<sup>19</sup> The ability of the deep CNN models has increased as the models used in the ImageNet dataset have become more complex since 2012, yet many are still not effective in terms of computing load. EfficientNet model, which is among the state-of-the-art models by reaching 84.4% accuracy with 66 M parameter in the ImageNet classification problem, consists of 8 models between B0 and B7, and as the model number grows the accuracy shows notable development while the number of calculated parameters show little increase, making it “efficient”.<sup>17</sup> The goal of deep learning architectures has so far been to build a smaller model with efficiently approaches yet shows decent accuracy, and Efficient Net has proved to show promising performances in medical fields such as well tackled tasks dealing with diabetic retinopathy<sup>20</sup>, skin lesions<sup>21</sup>, breast cancer<sup>22</sup>, osteoporosis<sup>23</sup> to recent problems such as COVID-19 diagnosis<sup>24</sup>. With the advent of future deep learning algorithms, tasks such as root and canal anatomy classification may become a tangible portion within everyday dental treatment.

In this study, both Grad-CAM and guided Grad-CAM was used to add explainability to the model. Most CAMs highlighted the apical 1/3 of the root where the canals showed convergence as in most C-shaped canals, yet some localized other areas such as the cemento-enamel junction or pulp chamber area. This may be because in most C-shaped canal cases the canal orifices tend to be closer to each other, giving in some cases a distinct shape compared to non-C shaped canal cases. There were no heat maps located outside of the tooth area, allowing us to confirm that the algorithm has at least used safe and meaningful prediction strategies rather than following the so-called Clever Hans predictors<sup>25 26</sup>. Heat maps focused upon areas apart from the apical 1/3 of the root were more frequently shown in the radiographic type II C shaped canal following the classification of Fan et al.<sup>27</sup> This is because the type II C shaped canal shows that the mesial and distal canals assume their own individual course to the apex, thus looking similar to a non-C shaped case in the periapical or panoramic radiograph. These misclassified heat maps also imply overfitting of the model. More data is needed to ensure increased accuracy and transparency.

There are notable limitations in this study. First, the sample size used in this study was relatively small compared to other CNN related studies. This was due to the limitation from that the radiographic images were obtained from patients who had visited the dental clinic for mandibular third molar extraction and thus the patients

enrolled for data collection were limited. The number of images prepared in this study was multiplied after data augmentation; nonetheless, the quantity of training dataset used in this study may still be considered insufficient. Although it is known that deep CNN algorithms such as Efficient Net are highly useful in cases where available training sets are limited, small datasets can be a bottleneck to further advancement of computer aided detection.<sup>28</sup> For high AI performance, using a high-quality training dataset is crucial, and this can be achieved by implementing high quality, well annotated datasets. Second, data homogeneity was present because the data was collected from one institution. Although pre-trained deep CNN models using large image datasets are effective for general image classification owing to their pre-trained weights, the possibility of overfitting cannot be excluded with a small dataset with a singular character coming from a limited data source. External validation is needed to confirm the multicenter studies are necessary for increased accuracy of the DL classification and diagnosis. Overall, overfitting should not be neglected. Third, because we handpicked Efficient Net among many available deep learning algorithms, it is important to keep up with the development other CNN algorithms. A different model using the same dataset shows different diagnostic outcomes as a result of variations in the CNN structure. New CNN algorithms differing in depth, width, or modified stratification methods are being developed continually, and it is important to consider these developments

in future studies. Last, the root figures were classified into only two categories; C shaped or non-C shaped. However, the root or canal morphology of the mandibular second molar can be subdivided to many categories. The non-C shaped canals can have either 2 or 3 roots, and although not commonly found, even C shaped canals can be present in a two rooted second molar, or a 1 rooted second molar can have a conical or O-shaped canal instead of the prevalent C-shaped canal. <sup>29</sup> Such variables, along with age, sex, or population-related morphological variations may possibly be implemented for advances in accurate diagnosis and classification.

In this study EfficientNet could accurately classify a mandibular second molar having a C-shaped canal morphology. Within the limitations of this study, we have developed and validated of a visually explainable deep learning CNN model for detection of C-shaped canals of the mandibular second molars in dental radiographs. Further studies are needed, but the results of this study may play an important role in C-shape canal prediction in the clinical and educational field of dentistry. Furthermore, by expanding the field of this model to various anatomic variations on all teeth, it is expected to aid in both the clinical and educational field as an explainable model, and can be as an explainable model, and can be developed to a deeper level through real world data feedback. (Figure 4.)

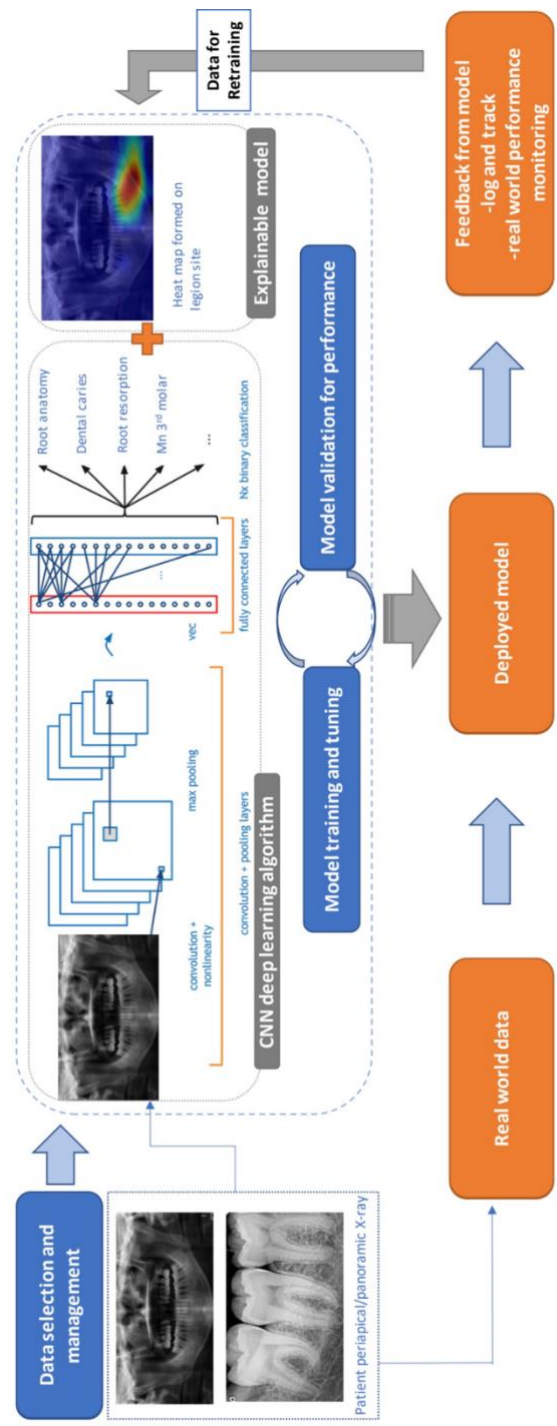


Figure 4. An overview of the expanded deep learning model and feedback process from real world data.

## **5. Conclusion**

The deep CNN algorithm model showed high accuracy in predicting the C-shaped canal variation among mandibular second molars. With further optimization of the test data using a larger dataset and improvements made in the model, a deep learning system can be expected to effectively diagnose C-shaped canals and aid clinicians in everyday practice.

## 6. References

1. Cooke HG, Cox FL. C-shaped canal configurations in mandibular molars. The Journal of the American Dental Association 1979;99(5):836-39.
2. Vertucci FJ. Root canal anatomy of the human permanent teeth. Oral Surgery, Oral Medicine, Oral Pathology and Oral Radiology 1984;58(5):589-99.
3. Endres MG, Hillen F, Salloumis M, et al. Development of a deep learning algorithm for periapical disease detection in dental radiographs. Diagnostics 2020;10(6):430.
4. Zhang R, Wang H, Tian YY, et al. Use of cone-beam computed tomography to evaluate root and canal morphology of mandibular molars in Chinese individuals. International endodontic journal 2011;44(11):990-99.
5. Gulabivala K, Aung T, Alavi A, et al. Root and canal morphology of Burmese mandibular molars. International endodontic journal 2001;34(5):359-70.
6. Haddad GY, Nehme WB, Ounsi HF. Diagnosis, classification, and frequency of C-shaped canals in mandibular second molars in the Lebanese population. Journal of endodontics 1999;25(4):268-71.
7. Helvacioglu-Yigit D, Sinanoglu A. Use of cone-beam computed tomography to evaluate C-shaped root canal systems in mandibular second molars in a Turkish subpopulation: a retrospective study. International Endodontic Journal 2013;46(11):1032-38.

8. Plotino G, Tocci L, Grande NM, et al. Symmetry of root and root canal morphology of maxillary and mandibular molars in a white population: a cone-beam computed tomography study in vivo. *Journal of endodontics* 2013;39(12):1545-48.
9. Manning S. Root canal anatomy of mandibular second molars: Part II C-shaped canals. *International endodontic journal* 1990;23(1):40-45.
10. Torabinejad M, Kutsenko D, Machnick TK, et al. Levels of evidence for the outcome of nonsurgical endodontic treatment. *Journal of Endodontics* 2005;31(9):637-46.
11. Scarfe WC, Farman AG. What is cone-beam CT and how does it work? *Dental Clinics of North America* 2008;52(4):707-30.
12. Lee J-H, Kim D-H, Jeong S-N, et al. Detection and diagnosis of dental caries using a deep learning-based convolutional neural network algorithm. *Journal of dentistry* 2018;77:106-11.
13. Krois J, Ekert T, Meinhold L, et al. Deep learning for the radiographic detection of periodontal bone loss. *Scientific reports* 2019;9(1):1-6.
14. Lee K-S, Jung S-K, Ryu J-J, et al. Evaluation of Transfer Learning with Deep Convolutional Neural Networks for Screening Osteoporosis in Dental Panoramic Radiographs. *Journal of Clinical Medicine* 2020;9(2):392.

15. Lee K, Kwak H, Oh J, et al. Automated Detection of TMJ Osteoarthritis Based on Artificial Intelligence. *Journal of Dental Research* 2020;99(12):1363-67.
16. Grad-cam: Visual explanations from deep networks via gradient-based localization. *Proceedings of the IEEE international conference on computer vision*; 2017.
17. Efficientnet: Rethinking model scaling for convolutional neural networks. *International Conference on Machine Learning*; 2019. PMLR.
18. Schwendicke F, Samek W, Krois J. Artificial Intelligence in Dentistry: Chances and Challenges. *Journal of Dental Research* 2020:0022034520915714.
19. Duong LT, Nguyen PT, Di Sipio C, et al. Automated fruit recognition using EfficientNet and MixNet. *Computers and Electronics in Agriculture* 2020;171:105326.
20. Deep-Learning-Based Early Detection of Diabetic Retinopathy on Fundus Photography Using EfficientNet. *Proceedings of the 2020 the 4th International Conference on Innovation in Artificial Intelligence*; 2020.
21. Skin Lesion Segmentation based on Integrating EfficientNet and Residual block into U-Net Neural Network. *2020 5th International Conference on Green Technology and Sustainable Development (GTSD)*; 2020. IEEE.

22. Wang J, Liu Q, Xie H, et al. Boosted EfficientNet: Detection of Lymph Node Metastases in Breast Cancer Using Convolutional Neural Network. arXiv preprint arXiv:201005027 2020
23. Yamamoto N, Sukegawa S, Kitamura A, et al. Deep Learning for Osteoporosis Classification Using Hip Radiographs and Patient Clinical Covariates. *Biomolecules* 2020;10(11):1534.
24. Marques G, Agarwal D, de la Torre Díez I. Automated medical diagnosis of COVID-19 through EfficientNet convolutional neural network. *Applied Soft Computing* 2020;96:106691.
25. Lapuschkin S, Wäldchen S, Binder A, et al. Unmasking clever hans predictors and assessing what machines really learn. *Nature communications* 2019;10(1):1-8.
26. Schwendicke F, Samek W, Krois J. Artificial intelligence in dentistry: chances and challenges. *Journal of dental research* 2020;99(7):769-74.
27. Fan B, Cheung GS, Fan M, et al. C-shaped canal system in mandibular second molars: part II—radiographic features. *Journal of endodontics* 2004;30(12):904-08.
28. Shin H-C, Roth HR, Gao M, et al. Deep convolutional neural networks for computer-aided detection: CNN architectures, dataset characteristics and transfer learning. *IEEE transactions on medical imaging* 2016;35(5):1285-98.

29. Kim S, Kim B, Kim Y. Mandibular second molar root canal morphology and variants in a Korean subpopulation. *International endodontic journal* 2016;49(2):136-44.

## 국문요약

치과 방사선 영상 내 C형 근관 판별 목적의 설명 가능한

딥러닝 모델 개발 및 검증

연세대학교 대학원 치의학과

양 수 진

지도교수 : 김 기 덕

목적 : 이 연구의 목적은 치과 방사선 사진을 사용하여 하악 제 2 대구치의 C형 근관을 감지하기 위한 시각적으로 설명 가능한 딥 러닝 모델을 개발하고 검증하는 것이다.

배경 : CNN (Convolution Neural Networks)은 컴퓨터 비전에서 탁월한 성능을 보여 왔으며 방사선 및 병리학 분야에서 질환의 탐지 및 분류 측면에서 유망한 결과를 낳았다. 또한 CNN 모델은 해석 가능해졌고 클래스 활성화 맵을 시각화하는 GRAD-CAM의 적용을 통해 설명 불가능성을 일정 수준까지 극복하였다.

치아의 치근 및 치아 근관계의 형태를 파악하는 것은 성공적인 수술적, 비수술적 근관치료를 위해 필수적이나 2차원 방사선 사진에서 이를 판단하는 것은 어려울 수 있으며 임상가의 경험과 숙달이 필요한 부분이다. 이는 특히 C형 근관을 보이는 하악 제2대구치에서 두드러진다. 하악 제2대구치의 C형 근관은 아시아인에서 10~45%로 많이 나타나는 형태학적 변이이며 그 복잡성으로 인해 해당 치아의 근관치료를 힘들게 하므로 술 전 이에 대한 평가가 필수적이다. C형 근관을 파악하지 않고 치료가 진행될 시 부족한 근관세정 및 성형에 따른 근관치료의 실패로 이어질 수 있으며, 치아의 예후 파악 및 환자에게 예후 고지에 불리할 수 있다.

치과 영역에서 통상적으로 진단에 사용할 수 있는 사진은 2차원의 파노라마 방사선 사진 또는 치근단 방사선 사진이며 CBCT를 찍는 것은

제한적이다. 이러한 제한된 영상 정보에서 C형 근관을 판단하는데 도움이 되는 장치가 있다면 임상 치료 영역, 또는 의료인 및 학생 교육 영역에서 유용할 것으로 판단된다.

이에 본 연구의 목적은 치과 방사선 사진을 이용하여 하악 제 2 대구치의 C자형 근관을 진단하기 위한 시각적으로 설명 가능한 딥 러닝 모델을 개발하고 검증하는 데 있다.

재료 및 방법 : 401 명의 환자로부터 1000 개의 하악 제 2 대구치의 치근단, 파노라마, CBCT 방사선 영상을 수집 하였다. 이미지 패치는 하악 제 2 대구치 영역의 치관부와 치근까지 모두 포함하게, 또는 치근 부분만 포함하도록 치근단 방사선 이미지 또는 파노라마 이미지로부터 준비하였다. (치관부-치근 그룹, 또는 치근 그룹으로 분류). 하악 제2 대구치에서 C형 근관 구성을 보이는지 여부를 확인하는 능력과 관련하여 근단 및 파노라마 방사선 사진을 사용한 딥 러닝 시스템의 진단 성능을 평가하였다. CBCT에서 나타난 근관 모양을 gold standard로 사용하였다. 학습 모델을 개발한 뒤 별도의 테스트 세트로 성능을 평가하였으며, 클래스 활성화 맵을 통해 모델이 결과를 얻기 위해 초점을 맞춘

부분을 평가하였다.

결과 : 6 개 그룹의 결과를 각각 얻어 비교하였다. 결과는 크게 두 그룹으로 나뉘었으며 이는 사용 된 이미지에 의해 치관과 치근을 모두 포함한 군과 (crown-root group) 치근 부분만을 포함한 군 (root only group)으로 구분되었다. 그런 다음 각 군을 사용 된 이미지 데이터의 소스로 나누었으며 이는 치근단 영상만을 이용한 경우 (peri), 파노라마 영상만을 이용한 경우 (panoramic) 또는 모든 영상 이미지를 이용한 경우 (both)로 구분되었다. C형 근관을 가진 하악 제 2 대구치는 47 %의 높은 유병률을 보였으며 전반적인 진단 정확도는 95 %로 나타났다. GRAD-CAM에서 얻은 히트 맵은 임상 의가 진단에 집중하는 영역과 일치하는 치근 중간부 1/3 에서 치근단부 1/3 까지의 영역에서 하이라이트를 보여주었다.

결론 : Deep CNN 알고리즘 모델은 하악 제 2 대구치 사이의 C형 근관 변화를 예측하는 데 높은 정확도를 보였다. 더 큰 데이터 세트를 사용하여 테스트 데이터를 추가로 최적화하고 모델을 개선하면 딥 러닝

시스템이 C형 근관을 효과적으로 진단하여 임상의의 일상적인 진료와 교육을 지원할 수 있을 것으로 기대된다.

---

키워드 : 인공 지능, 딥 러닝, 근관 형태, 하악 제 2 대구치, C형 근관